Supplementary Figures 1-11

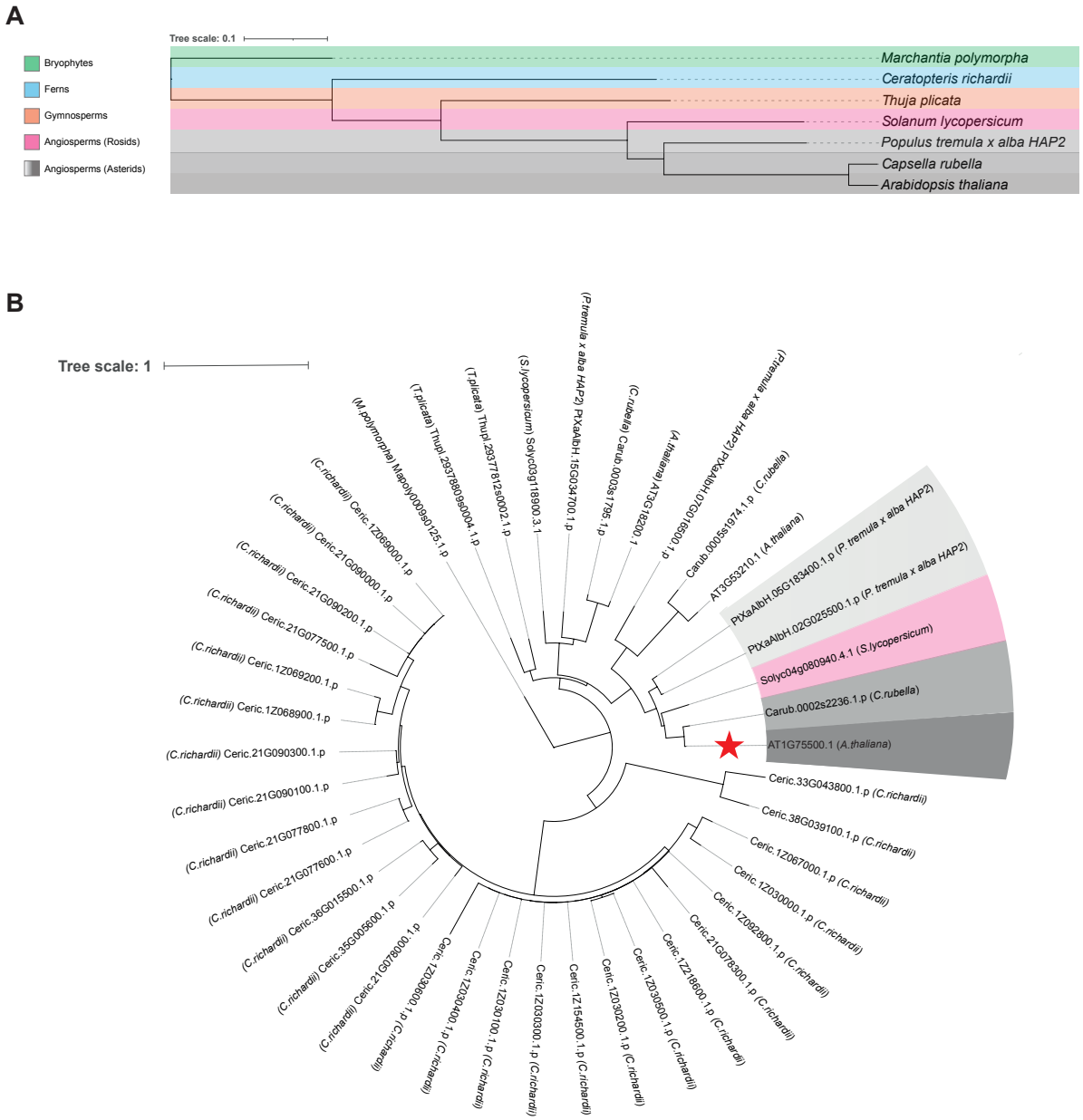

Supplementary Fig. 1. Phylogenetic analysis of the EamA/WAT protein family across representative land plants. A Species tree inferred by OrthoFinder from the complete proteomes of representative land plants, including the bryophyte *Marchantia polymorpha*, the fern *Ceratopteris richardii*, the gymnosperm *Thuja plicata*, and representative angiosperms (*Solanum*

lycopersicum, *Populus tremula* × *alba*, *Capsella rubella*, and *Arabidopsis thaliana*). Colored backgrounds indicate the major taxonomic groups included in the analysis. **B** Gene tree of the WAT1-like protein family inferred by OrthoFinder. The shaded sector highlights the conserved angiosperm WAT1 clade, which includes the functionally characterized WAT1 proteins from *Arabidopsis thaliana* and *Solanum lycopersicum*, along with the two *Populus tremula* × *alba* paralogues, WAT1 (PtXaAlbH.05G183400) and WAT2 (PtXaAlbH.02G025500). The red star denotes *Arabidopsis thaliana* WAT1 (AT1G75500). Scale bars indicate substitutions per site.

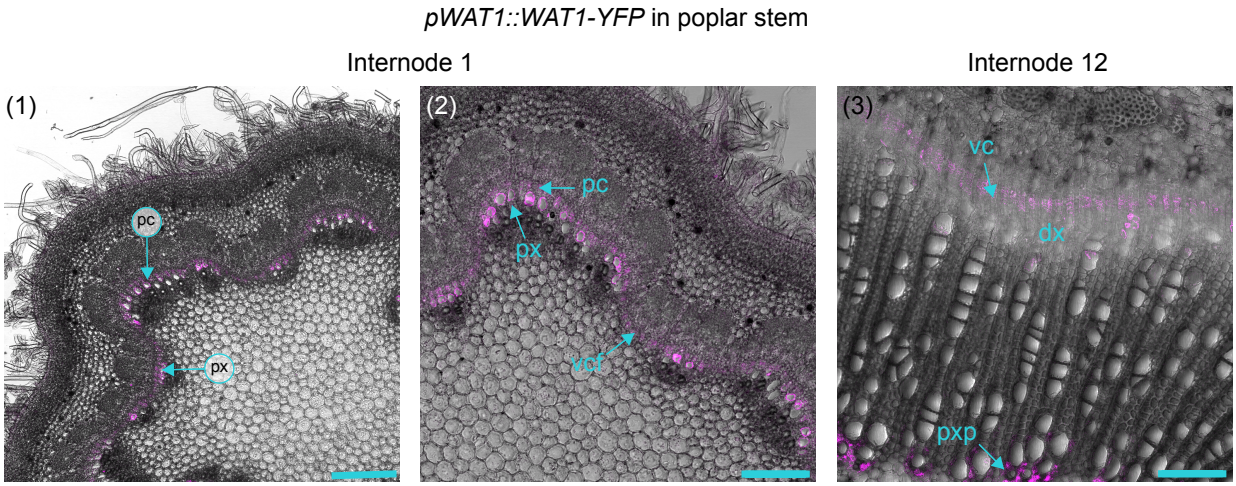

Supplementary Fig. 2. WAT1 is localizes throughout vascular development in poplar stems. Localization of p*WAT1*::*WAT1*-YFP in transgenic poplar stems. Representative confocal images of stem transverse sections at internode 1 (1-2) and internode 12 (3). YFP fluorescence (magenta) was detected in vascular tissues, including procambial cells, primary xylem, vascular cambium, and developing xylem. Abbreviations: dx, developing xylem; pc, procambium; px, primary xylem; vcf, vascular cambial founder cells; v, vessel; vc, vascular cambium; Scale bars, 190 μm (1), 140 μm (2), 150 μm (3).

p35S::WAT2-eGFP

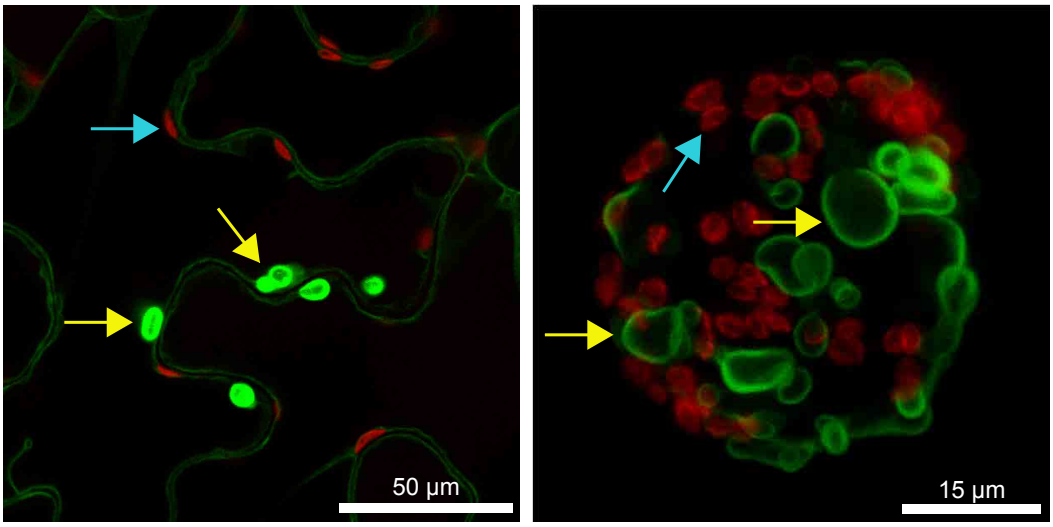

*p35S::WAT2-**m**GFP*

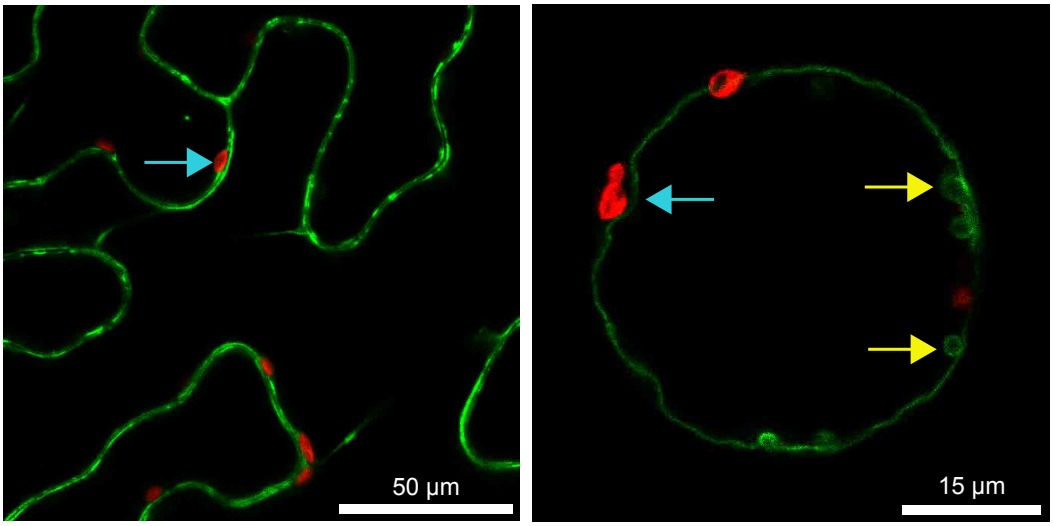

*p35S::WAT1-**m**GFP*

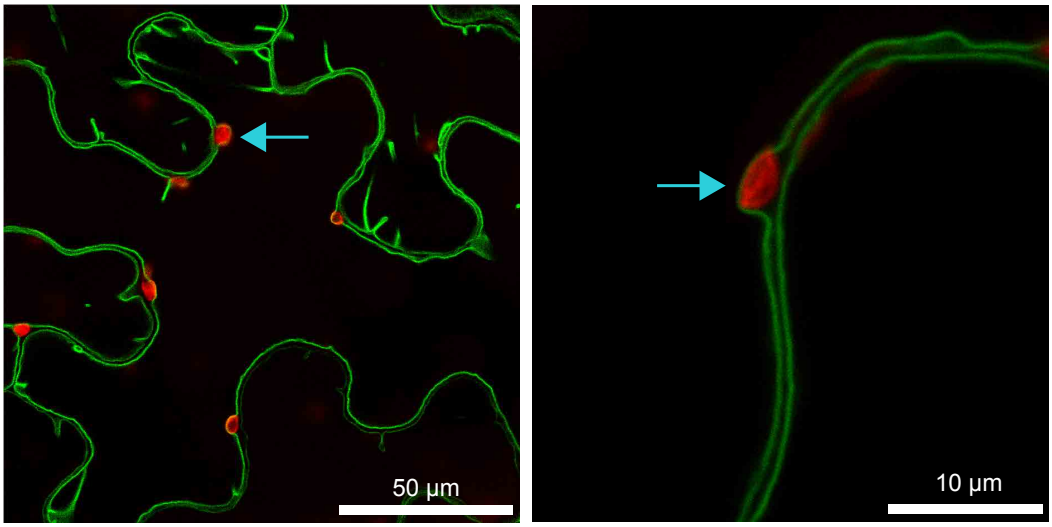

Supplementary Figure 3. WAT1 and WAT2 are localized at the tonoplast in *Nicotiana benthamiana* epidermal cells. Representative confocal images of *Nicotiana benthamiana* epidermal cells and isolated protoplasts transiently expressing *35S::WAT2-eGFP*, *35S::WAT2-mGFP*, or *35S::WAT1-mGFP*. WAT2 fused to eGFP frequently induced prominent tonoplast bulbs (yellow arrows), whereas replacement of eGFP with the monomeric GFP variant (mGFP) markedly reduced bulb formation while preserving membrane-associated fluorescence. Chloroplast autofluorescence is indicated by cyan arrows and was used as a positional reference. Scale bars, 50 μm (left panels), 15 μm (upper and middle right panels), and 10 μm (lower right panel).

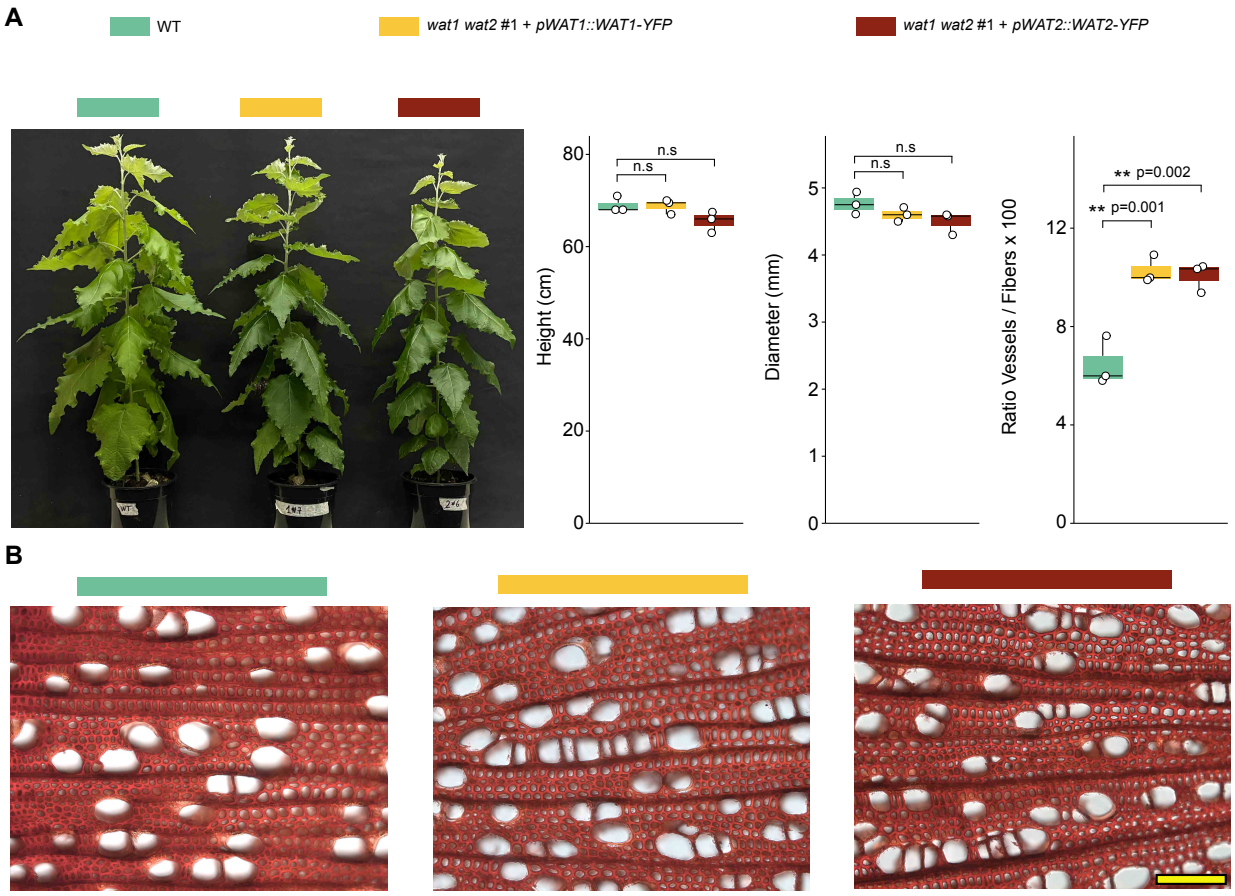

Supplementary Fig. 4. Either WAT1 or WAT2 is sufficient to restore normal vegetative growth in the *wat1 wat2* mutant. A Representative WT and *wat1 wat2* plants complemented with either *pWAT1::WAT1-YFP* or *pWAT2::WAT2-YFP*. Expression of either WAT1 or WAT2 under its native promoter restored plant height and stem diameter to WT levels, whereas the vessel-to-fiber ratio was only partially restored. Data are presented as the mean ± SE, with individual biological replicates shown as dots. Statistical significance was determined by one-way ANOVA followed by Dunnett's post hoc test comparing each complemented line with WT (n.s., not significant; **P < 0.01). **B** Representative transverse sections of mature stems showing the secondary xylem of WT and *wat1 wat2* plants complemented with either *pWAT1::WAT1-YFP* or *pWAT2::WAT2-YFP*. Scale bar, 100 µm.

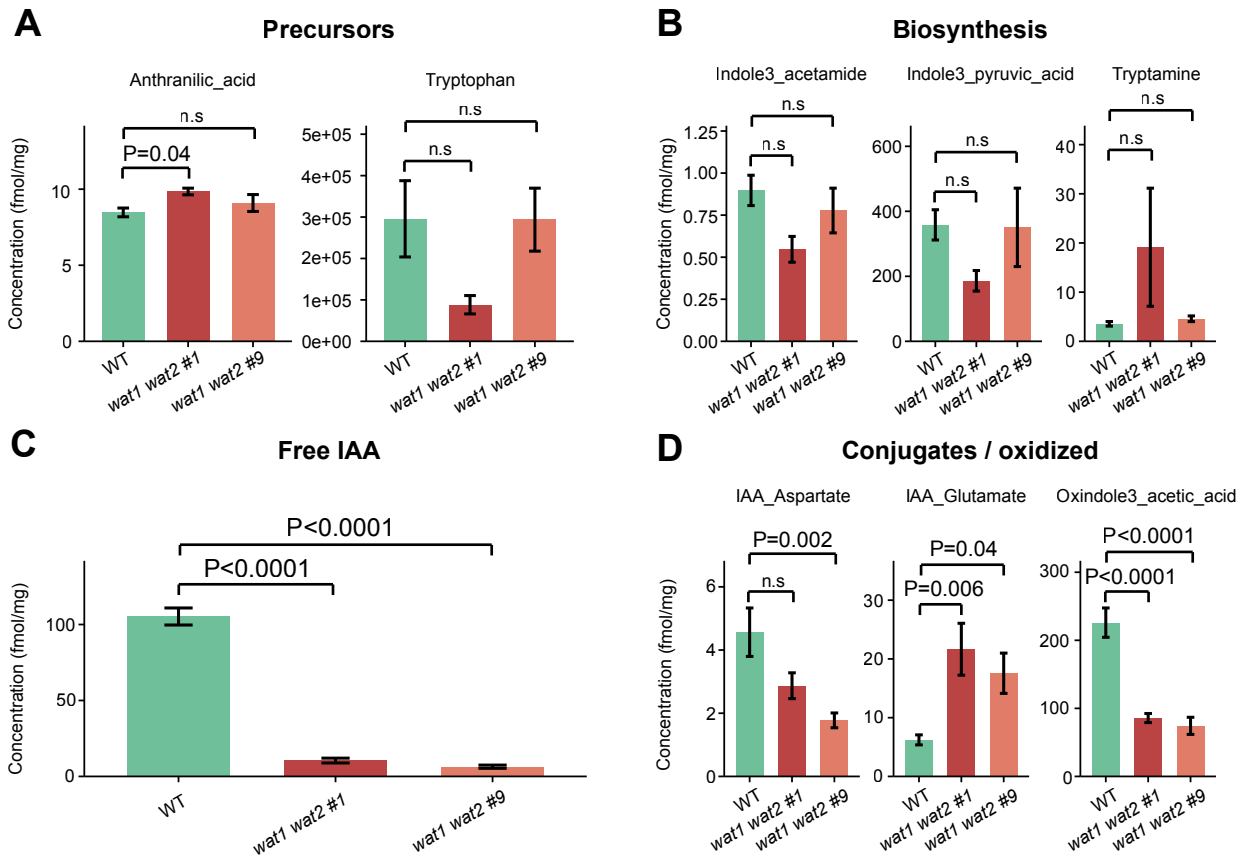

Supplementary Fig. 5. WAT1 and WAT2 are required to maintain free IAA homeostasis in poplar stems. Quantification of auxin precursors, biosynthetic intermediates, free IAA, auxin conjugates, and oxidized auxin metabolites in developing stems of WT and two independent *wat1 wat2* mutant lines (*wat1 wat2* #1 and *wat1 wat2* #9). **A** Auxin precursors anthranilic acid and tryptophan. **B** Auxin biosynthetic intermediates indole-3-acetamide, indole-3-pyruvic acid, and tryptamine. **C** Free IAA levels were strongly reduced in both *wat1 wat2* mutant lines compared with WT. **D** Auxin conjugates and oxidized metabolites. IAA-Glu levels were increased, whereas oxIAA levels were strongly reduced in both mutant lines. Data are presented as mean ± SE (n = 8 biological replicates per genotype). Statistical significance was determined by one-way ANOVA followed by Dunnett's post hoc test comparing each mutant line with WT. n.s., not significant. Exact P values are shown for significant comparisons.

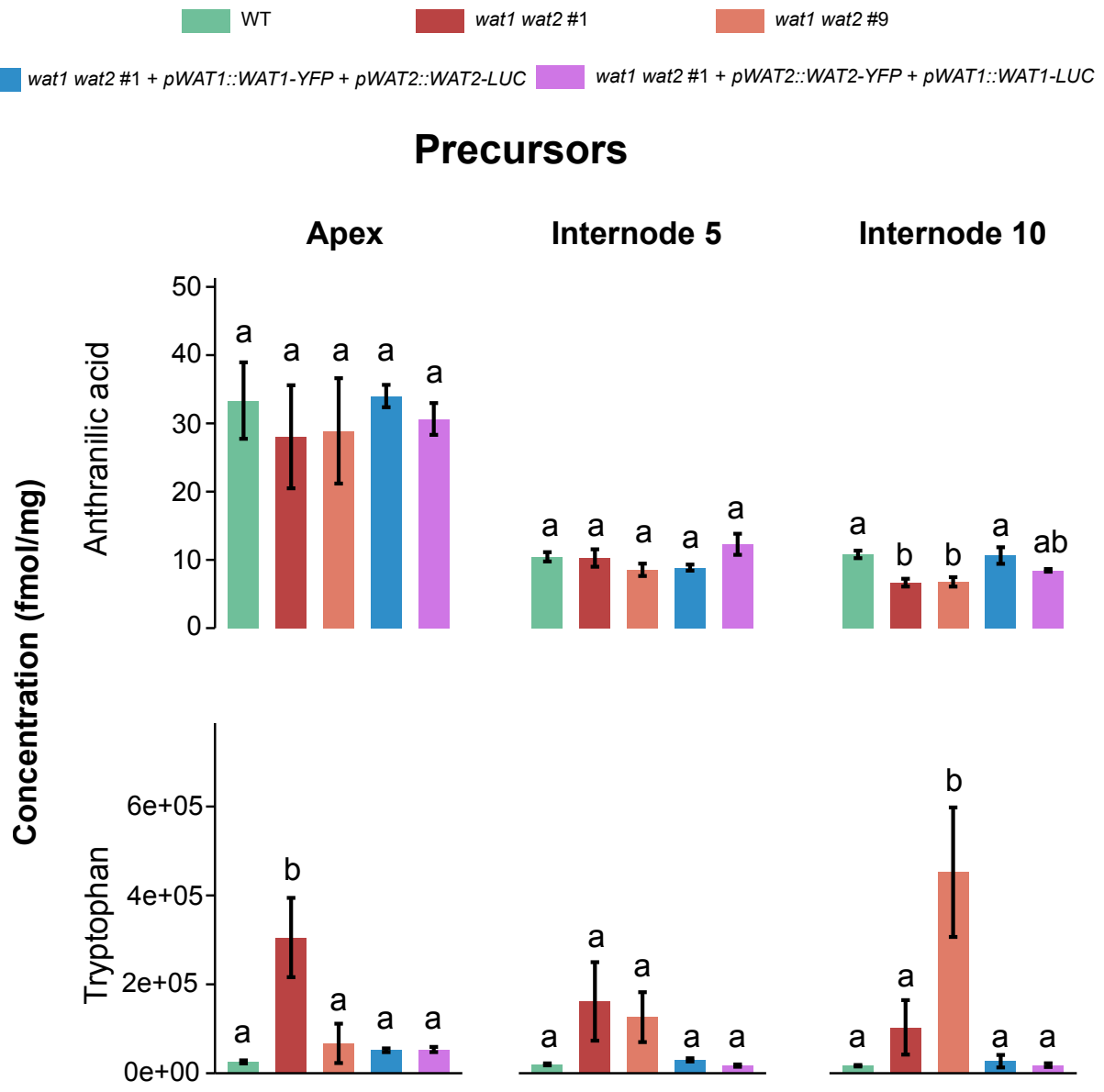

Supplementary Fig. 6. WAT1 and WAT2 regulate free IAA homeostasis rather than auxin biosynthesis. Quantification of auxin precursors in the shoot apex, internode 5, and internode 10 of WT, two independent *wat1 wat2* mutant lines (*wat1 wat2*#1 and *wat1 wat2*#9), and complemented lines expressing *pWAT1*::*WAT1*-YFP + *pWAT2*::*WAT2*-LUC or *pWAT2*::*WAT2*-YFP + *pWAT1*::*WAT1*-LUC in the *wat1 wat2* #1 background. The early precursor anthranilic acid showed only modest reductions in specific mutant tissues; however, these changes were not accompanied by a corresponding decrease in tryptophan, which remained largely unchanged between WT and mutant plants and even accumulated in specific tissues, indicating that these

changes do not explain the extreme reduction of free IAA in the stem of mutant trees. Data are presented as mean ± SE (WT and *wat1 wat2* mutant lines, n = 4 biological replicates; complemented lines, n = 3 biological replicates). Different letters indicate statistically significant differences (one-way ANOVA followed by Holm's post hoc test ($P < 0.05$).

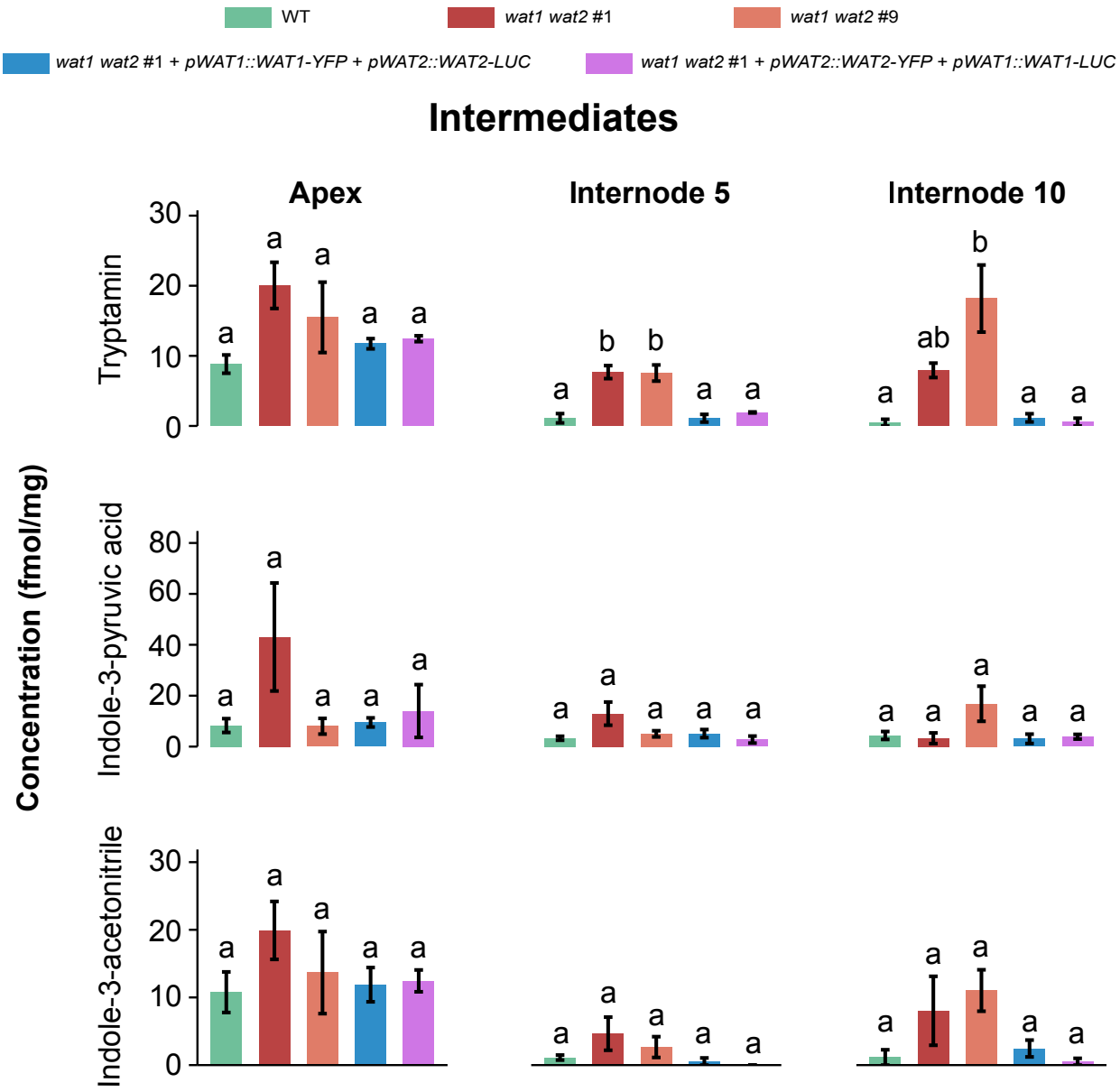

Supplementary Fig. 7. WAT1 and WAT2 regulate free IAA homeostasis rather than auxin biosynthesis. Quantification of auxin biosynthetic intermediates in the shoot apex, internode 5, and internode 10 of WT, two independent *wat1 wat2* mutant lines (*wat1 wat2*#1 and *wat1 wat2*#9), and complemented lines expressing *pWAT1*::*WAT1*-YFP + *pWAT2*::*WAT2*-LUC or *pWAT2*::*WAT2*-YFP + *pWAT1*::*WAT1*-LUC in the *wat1 wat2* #1 background. Tryptamine, indole-3-pyruvic acid, and indole-3-acetonitrile levels showed no consistent differences among genotypes across the three stem regions, indicating that WAT mutations have little effect on auxin biosynthesis. Data are presented as mean ± SE (WT and *wat1 wat2* mutant lines, n = 4 biological replicates;

complemented lines, n = 3 biological replicates). Different letters indicate statistically significant differences (one-way ANOVA followed by Holm's post hoc test ($P < 0.05$).

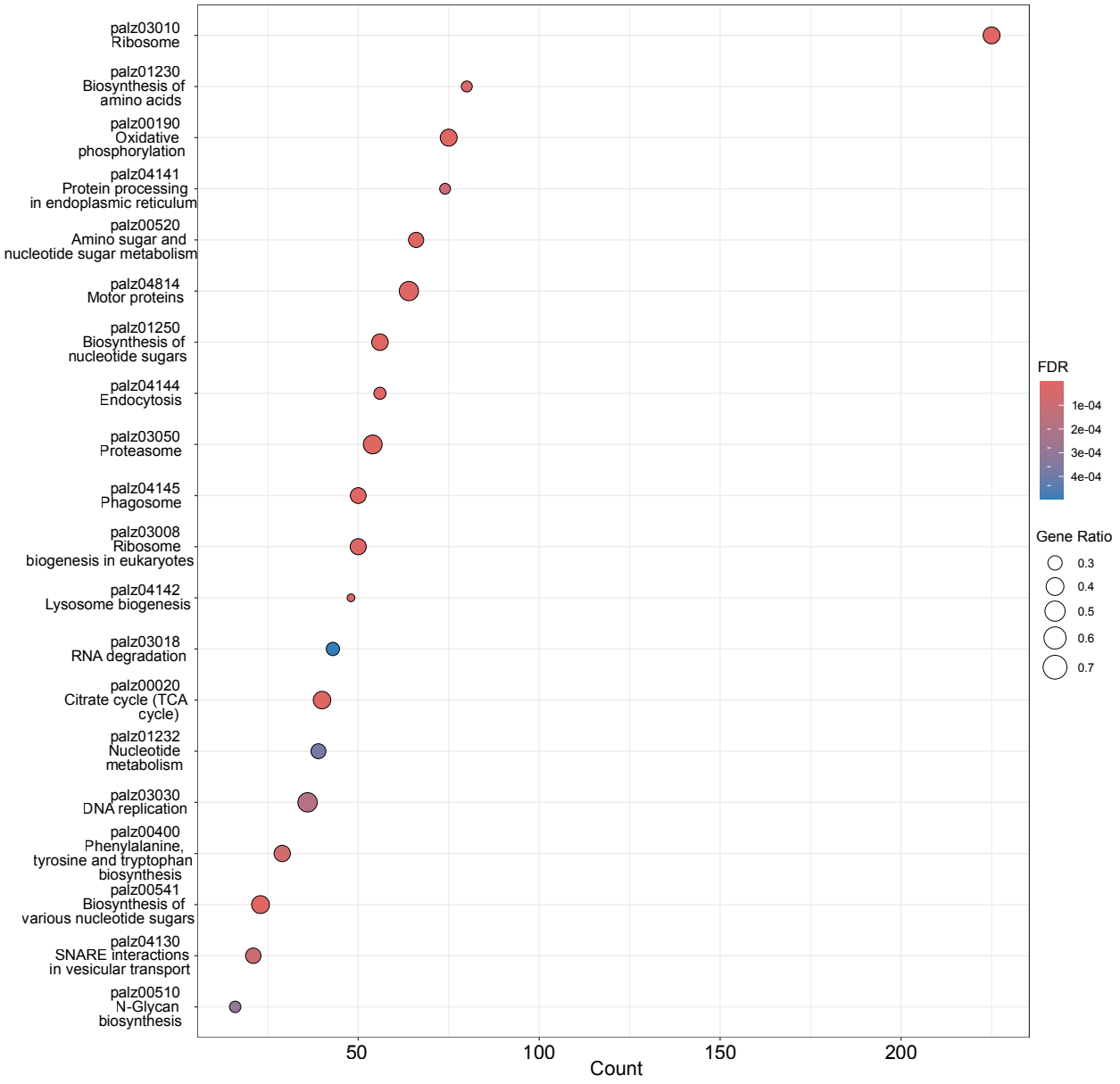

Supplementary Fig. 8. GSEA of repressed pathways in *wat1 wat2* stems. Dot plot showing the top 20 pathways repressed in *wat1 wat2* mutants, identified by one-tailed negative Gene Set Enrichment Analysis (GSEA) using differential expression results from the bulk RNA-seq dataset. Pathway names and their corresponding *Populus* KEGG identifiers are shown on the y-axis, whereas the x-axis indicates the number of genes from the enriched gene set assigned to each pathway (Count). Dot size represents the Gene Ratio, calculated as the proportion of enriched genes relative to the total number of genes in each pathway, and dot color indicates the false discovery rate (FDR).

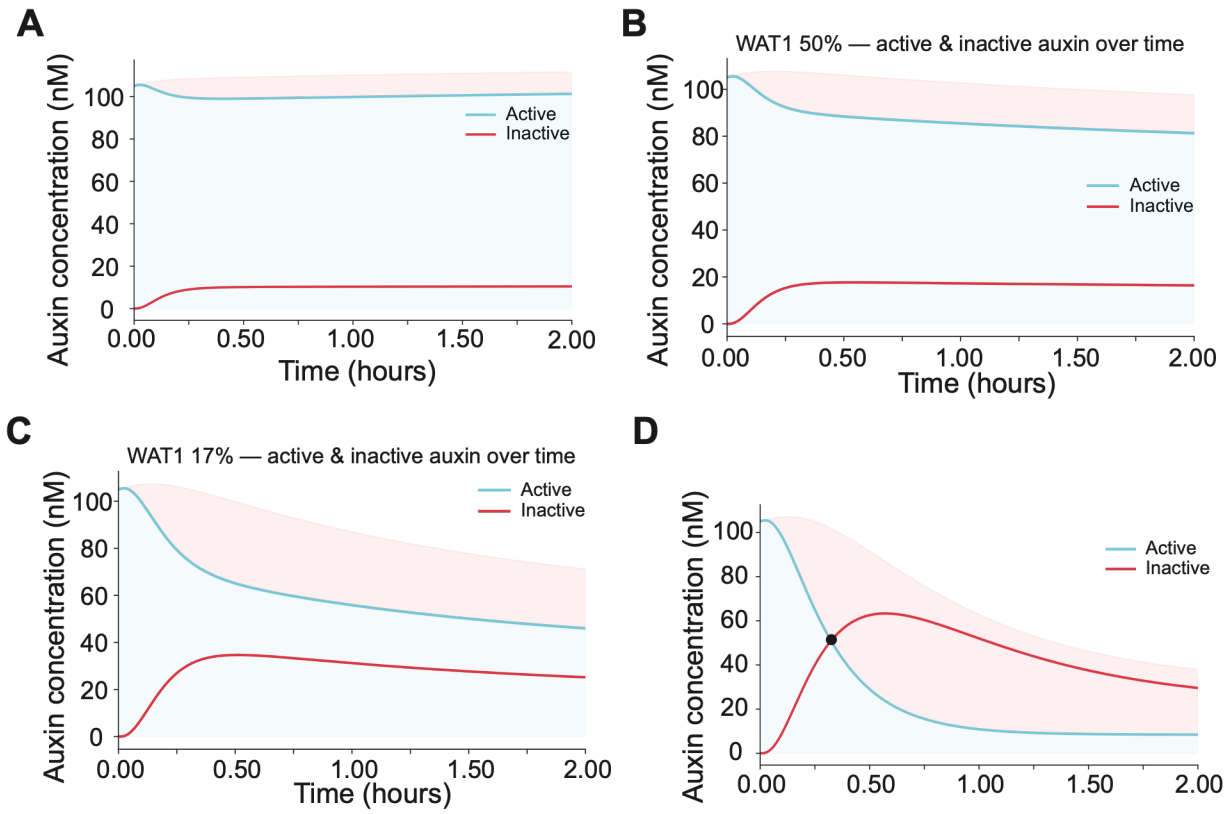

Supplementary Fig. 9. Simulation of WAT gene dosage on fractioning of active and inactive auxin in the cell. A-D Predicted kinetics of active (blue curve) and inactive (red curve) auxin concentration in WT-like scenario(A), ½ reduction in WAT gene expression (B), and *wat* mutant(D).

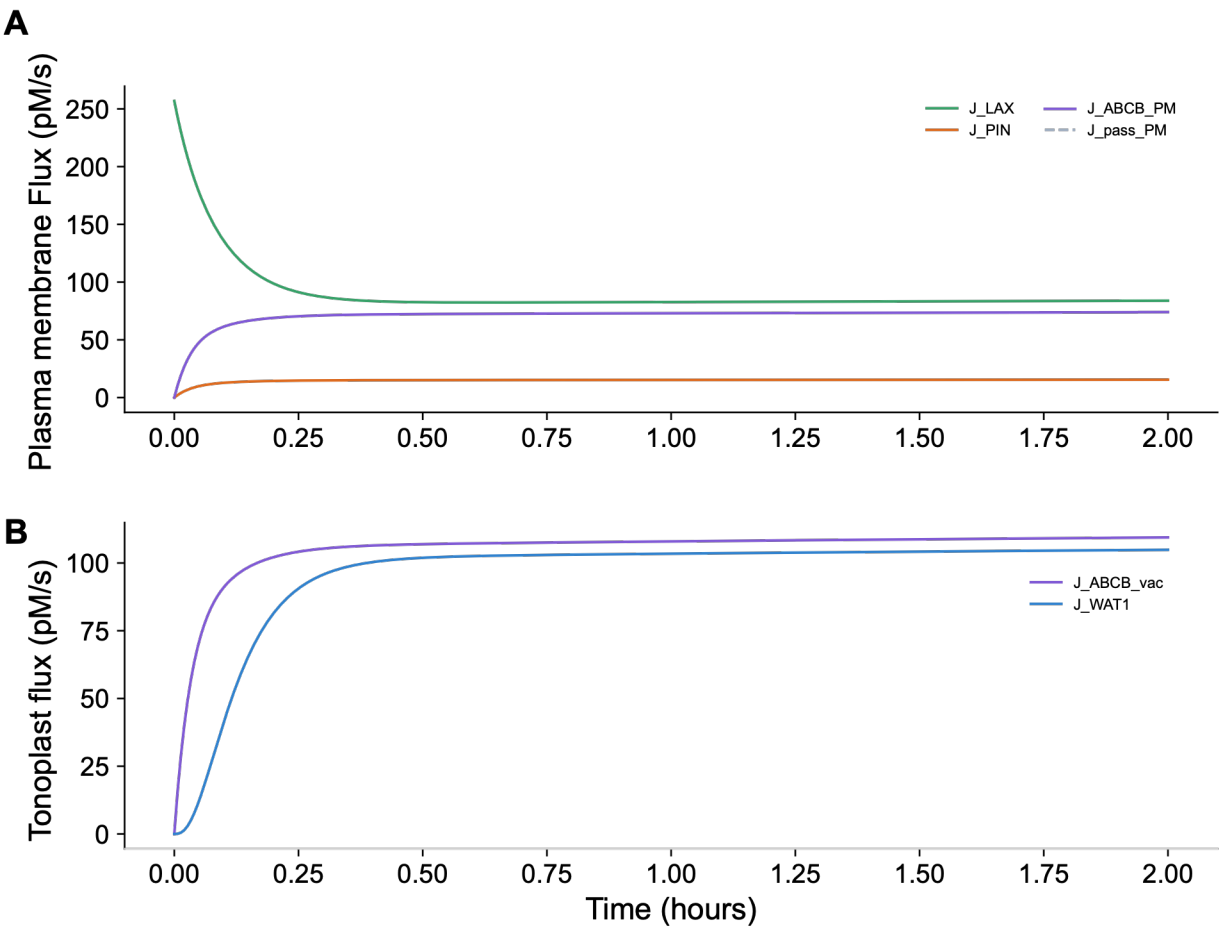

Supplementary Fig. 10. Dynamics of auxin fluxes in WT-like simulation. A Plasma membrane associated fluxes are initially dominated by active influx and later equalized by efflux from the cell. **B** Vacuole-associated fluxes show an initial delay in auxin release from the vacuole, indicating a capacity to store auxin and controlled release.

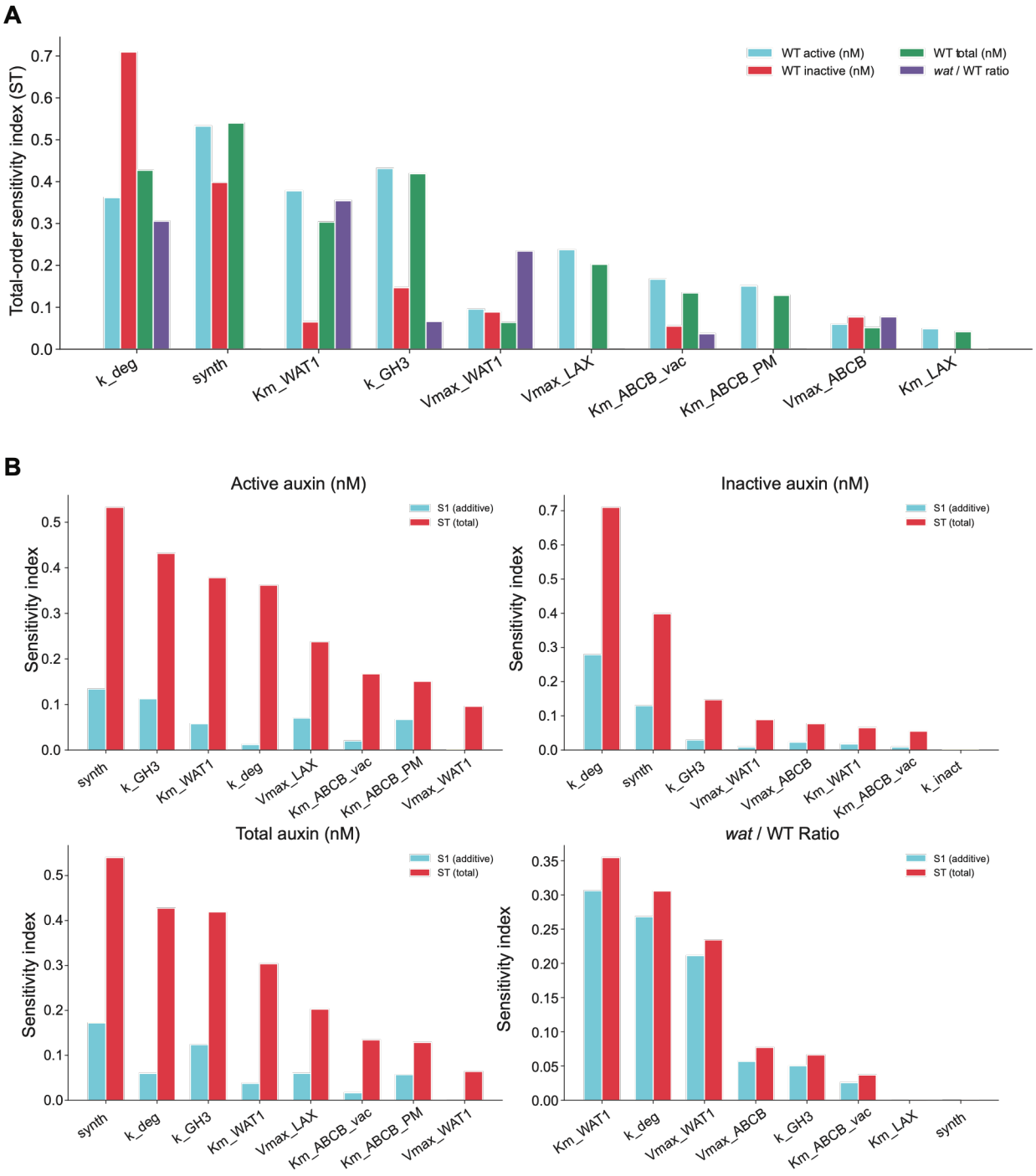

Supplementary Fig. 11. Global sensitivity analysis of the model. A The global sensitivity analysis reveals the important role for intracellular auxin homeostasis in maintaining balance between active and inactive auxin. B Local versus global sensitivity to transport and metabolism related parameters.

Supplementary Tables 12-16

Gen	Primers qPCR (5’ - 3’)	
AFB2 (PtXaAlbH.05G121200)	fwd	GGAAATTAAATCTTGCAGGT
	rev	AGGGCTTCTGGATTGAATG
ARF3 (PtXaAlbH.04G039300)	fwd	TCTGCAACATCATCCCG
	rev	CTTTCACACAAGCTAATACG
ARF8 (PtXaAlbH.04G064100)	fwd	TGTGGCTTAAGACCCTGC
	rev	GAAGAATGCCATGCAGCTC
DAHPS2 (PtXaAlbH.05G123400)	fwd	AGCCAAGGTTAAGACTGC
	rev	AATGTCCGCCTCTTCCTT
QUASIMODO2 (PtXaAlbH.05G124100)	fwd	CCACAACTCTCAGAAGCC
	rev	CTTCTCATTTGCTCAGCACC
SK (PtXaAlbH.07G068300)	fwd	TGTATCCAGTATCACACCTG
	rev	GAAATAGAATCCCATTGCAGC
UBQ7 (PtXaAlbH.05G152100)	fwd	GGAACGGGTTGAGGAGAAAGAAG
	rev	GCAAGAACAAGATGAAGCACAGAGC

Supplementary Table 12. Primer sequences used in this study. List of primer sequences used for RT-qPCR analyses performed in this study, including gene-specific primers used for transcript quantification.

Genotype	Stem diameter only with the secondary xylem (mm)
WT rep.1	7.17
WT rep.2	6.31
WT rep.3	6.40
WT rep.4	6.53
WT rep.5	6.76
wat1 wat2 #1 rep.1	7.76
wat1 wat2 #1 rep.2	6.47
wat1 wat2 #1 rep.3	7.13
wat1 wat2 #1 rep.4	6.74
wat1 wat2 #1 rep.5	5.86
wat1 wat2 #1 rep.6	6.39
wat1 wat2 #1 rep.7	6.03
wat1 wat2 #1 rep.8	6.42
wat1 wat2 #1 rep.9	5.92
wat1 wat2 #1 rep.10	5.86

Supplementary Table 13. Secondary xylem diameter of stems used for secondary cell wall analyses. Diameter of the secondary xylem measured in the basal stems of WT and *wat1 wat2* plants used for secondary cell wall composition analyses. Plants were harvested after reaching a comparable degree of secondary xylem development to minimize developmental differences between genotypes. Each point represents one biological replicate.

Transporter	Abundance (a.u.)	Vmax ($\mu M \cdot s^{-1}$)	Km (µM)	Reference
AUX1/LAX (PM influx)	2.97	0.0027	1.0 (upper bound)	Yang et al. (2006)[1], Rubery, P.H. & Sheldrake, A.R. (1974)[2].
PIN (PM efflux)	3.77	0.0034	10.0	Petrasek et al. (2006)[3]
ABCB1/19 (PM efflux)	2.77	0.0025	1.5(upper bound)	Geisler et al. (2005)[4], Blakeslee, J.J. et al. (2007)[5].
ABCB-like (tono import)	2.77	0.0025	1.0	Estimated
WAT1 (tono export)	6.96	0.0063	0.6	Grid-search
k_{inact}	0.00458	s^{-1}	Active to inactive in vacuole	Grid-search
k_{deg}	0.000420	s^{-1}	Inactive degradation in vacuole	Grid-search
k_{GH3}	0.0001	s^{-1}	GH3-mediated conjugation	Grid-search
synth	9.748e-06	$\mu M \cdot s^{-1}$	Basal synthesis rate	Grid-search
P_{IAH_PM}	8.0×10^{-4}	s^{-1}	PM passive permeability	Gutknecht & Walter (1980)[6]
P_{IAH_tono}	2.0×10^{-5}	s^{-1}	Tonoplast passive permeability	Estimated

SCALE	0.00091	μM·s⁻¹/a.u.	Global Vmax scaling factor	Grid-search

Supplementary Table 14. Measured and adjusted model parameters.

References for the Supplementary Table 14

1. Yang, Y., Hammes, U. Z., Taylor, C. G., Schachtman, D. P. & Nielsen, E. High-Affinity Auxin Transport by the AUX1 Influx Carrier Protein. *Current Biology* **16**, 1123–1127 (2006).
2. Rubery, P. H. & Sheldrake, A. R. Carrier-mediated auxin transport. *Planta* **118**, 101–121 (1974).
3. Petrášek, J. *et al.* PIN Proteins Perform a Rate-Limiting Function in Cellular Auxin Efflux. *Science* **312**, 914–918 (2006).
4. Geisler, M. *et al.* Cellular efflux of auxin catalyzed by the Arabidopsis MDR/PGP transporter AtPGP1. *The Plant Journal* **44**, 179–194 (2005).
5. Blakeslee, J. J. *et al.* Interactions among PIN-FORMED and P-Glycoprotein Auxin Transporters in *Arabidopsis*. *The Plant Cell* **19**, 131–147 (2007).
6. Gutknecht, J. & Walter, A. (1980). Transport of auxin through lipid bilayer membranes. J Membr Biol, 56(1), 65-72.

Genotype	Active (nM)	Active Experiment	Inactive (nM)	Inactive Experiment	Apo (nM)	Cyt (nM)	Vac Act (nM)	Vac Inact (nM)
WT	105.3	105.0	10.9	10.8	33.3	47.2	24.8	10.9
wat	8.4	8.4	22.2	22.0	2.6	3.7	2.0	22.2

Supplementary Table 15. Predicted WT vs Mutant auxin profiles along experimental measurements.

Genotype	Active (nM)	Inactive (nM)	Total (nM)	Apo (nM)	Cyt (nM)	Vac Act (nM)	Vac Inact (nM)	Rel. Active
Wild type (WT)	105.3	10.9	116.2	33.3	47.2	24.8	10.9	1.000
wat1	8.4	22.2	30.6	2.6	3.7	2.0	22.2	0.080
pin	99.4	10.9	110.2	27.4	47.2	24.8	10.9	0.944
aux1 lax	601.2	10.9	612.1	529.2	47.2	24.8	10.9	5.709
abcb double	99.2	0.0	99.2	10.6	88.6	0.0	0.0	0.942
gh3	230.7	23.2	254.0	74.2	104.5	52.0	23.2	2.191

Supplementary Table 16. Forecasted auxin profiles in mutant simulations

Supplementary Movie Legends

Supplementary Movie 1. Dynamic visualization of WT-like simulation shows the changes in auxin profiles in the cell. Active auxin in blue and inactive in red. Cellular compartments are: outermost apoplast followed by cytosol and tonoplast (central rectangular).

Supplementary Movie 2. Dynamic visualization of *wat* mutant simulation shows the changes in auxin profiles in the cell. Active auxin in blue and inactive in red. Cellular compartments are: outermost apoplast followed by cytosol and tonoplast (central rectangular).